

## Article

# *MaNrtB*, a Putative Nitrate Transporter, Contributes to Stress Tolerance and Virulence in the Entomopathogenic Fungus *Metarhizium acridum*

Jia Wang<sup>1,2,3,4</sup>, Yuneng Zou<sup>1,2,3,4</sup>, Yuxian Xia<sup>1,2,3,4,\*</sup>  and Kai Jin<sup>1,2,3,4,\*</sup> 

<sup>1</sup> Genetic Engineering Research Center, School of Life Sciences, Chongqing University, Chongqing 401331, China; 202326021033@cqu.edu.cn (J.W.)

<sup>2</sup> Chongqing Engineering Research Center for Fungal Insecticide, Chongqing 401331, China

<sup>3</sup> Key Laboratory of Gene Function and Regulation Technologies Under Chongqing Municipal Education Commission, Chongqing 401331, China

<sup>4</sup> National Engineering Research Center of Microbial Pesticides, Chongqing 401331, China

\* Correspondence: yuxianxia@cqu.edu.cn (Y.X.); jinkai@cqu.edu.cn (K.J.)

**Abstract:** Nitrogen is an essential nutrient that frequently determines the growth rate of fungi. Nitrate transporter proteins (Nrts) play a crucial role in the cellular absorption of nitrate from the environment. Entomopathogenic fungi (EPF) have shown their potential in the biological control of pests. Thus, comprehending the mechanisms that govern the pathogenicity and stress tolerance of EPF is helpful in improving the effectiveness and practical application of these fungal biocontrol agents. In this study, we utilized homologous recombination to create *MaNrtB* deletion mutants and complementation strains. We systematically investigated the biological functions of the nitrate transporter protein gene *MaNrtB* in *M. acridum*. Our findings revealed that the disruption of *MaNrtB* resulted in delayed conidial germination without affecting conidial production. Stress tolerance assays demonstrated that the *MaNrtB* disruption strain was more vulnerable to UV-B irradiation, hyperosmotic stress, and cell wall disturbing agents, yet it exhibited increased heat resistance compared to the wild-type strain. Bioassays on the locust *Locusta migratoria manilensis* showed that the disruption of *MaNrtB* impaired the fungal virulence owing to the reduced appressorium formation on the insect cuticle and the attenuated growth in the locust hemolymph. These findings provide new perspectives for understanding the pathogenesis of EPF.

**Keywords:** entomopathogenic fungi; *Metarhizium acridum*; *MaNrtB*; stress tolerance; virulence



Academic Editors: Nicolás Pedrini and Jiaqin Xie

Received: 19 November 2024

Revised: 28 January 2025

Accepted: 30 January 2025

Published: 1 February 2025

**Citation:** Wang, J.; Zou, Y.; Xia, Y.; Jin, K. *MaNrtB*, a Putative Nitrate Transporter, Contributes to Stress Tolerance and Virulence in the Entomopathogenic Fungus *Metarhizium acridum*. *J. Fungi* **2025**, *11*, 111. <https://doi.org/10.3390/jof11020111>

**Copyright:** © 2025 by the authors. Licensee MDPI, Basel, Switzerland. This article is an open access article distributed under the terms and conditions of the Creative Commons Attribution (CC BY) license (<https://creativecommons.org/licenses/by/4.0/>).

## 1. Introduction

Numerous insect pests are prevalent in the natural environment, presenting significant challenges to agriculture, ecological balance, and human well-being [1]. Entomopathogenic fungi (EPF), a group of fungi that can cause infections and death in insects and other arthropods, have emerged as a promising and eco-friendly alternative to chemical insecticides and are extensively utilized as biocontrol agents against insect pests [2]. Well-known EPFs, such as *Metarhizium acridum* and *Beauveria bassiana*, have shown their potential and advantages in the biological control of pests within agricultural ecosystems [3]. Therefore, understanding the mechanisms that govern the pathogenicity and stress tolerance of EPF is helpful in improving the effectiveness and practical application of these fungal biocontrol agents.

In fungi, detecting and effectively utilizing nutrients are crucial for the successful establishment and rapid expansion of fungal colonies, and nitrogen, a critical nutrient,

often dictates the growth rate of fungi [4]. The metabolism of nitrogen sources encompasses a range of biochemical pathways and mechanisms, such as the assimilation of ammonia, the reduction of nitrates, the fixation of nitrogen, the synthesis of amino acids, and so on [5]. Within this metabolic network, nitrate metabolism is an important part of nitrogen source metabolism in fungi.

Nitrate transporter proteins (Nrts) are pivotal in the cellular uptake of nitrate from the surroundings, playing a critical role in the assimilation, metabolism, and utilization of nitrate. The genetic exploration of these transporters in eukaryotes began in 1991 with the discovery of the *CrnA* gene, which encodes a transmembrane protein, in *Aspergillus nidulans* [6]. The *CrnA*-deficient strains exhibited nitrate uptake defects in both the conidial and the mycelial growth phases [7]. These high-affinity transport systems are part of the nitrate/nitrite porter family, a unique subset within the major facilitator superfamily (MFS), the largest group of secondary transporters [8]. Most eukaryotic organisms possess multiple Nrt protein variants, each encoded by distinct genes [9]. For instance, in the yeast *Hansenula polymorpha* (syn *Ogataea angusta*), the *YNT1* mutants exhibits a deficiency in the uptake of nitrate [10]. In the pathogenic fungus *Fusarium oxysporum* f. sp. *Lycopersici*, the targeted deletion of the nitrate-transporting gene *Ntr1* significantly impairs fungal growth when nitrate serves as the nitrogen source [11]. Similarly, in *Ustilago maydis* (syn *Mycosarcoma maydis*), the growth of nitrate transporter protein mutants is hindered in media where nitrate is the sole nitrogen source and their pathogenicity is diminished [12]. *Trichoderma atroviride*, a prevalent plant growth-promoting fungus, has been shown to rely on the nitrate transporter CHL1 for nitrogen uptake in MS medium supplemented with  $\text{NH}_4\text{NO}_3$  [13]. Collectively, these findings underscore the influence of nitrate transporter proteins on fungal growth and pathogenicity. Despite their importance, the characterization of nitrate transporter genes in entomopathogenic fungi remains unexplored. Here, we investigated some biological processes that may be affected by the activity of a putative nitrate transporter, MaNrtB, in *M. acridum*.

## 2. Materials and Methods

### 2.1. Strains and Culture Conditions

The wild-type strain of *M. acridum* (WT) has been archived at the China General Microbiological Culture Collection Center (CGMCC) with the accession number 0877. In conducting the genetic engineering and fungal transformation for this study, we employed *Escherichia coli* DH5 $\alpha$  (Solarbio, Beijing, China) and *Agrobacterium tumefaciens* AGL1 (Solarbio, Beijing, China), respectively. The fungal strains employed in this investigation were cultivated on a modified Sabouraud dextrose agar medium, specifically a one-quarter-strength formulation (1/4 SDAY). This medium is composed of 1% dextrose, 0.25% mycological peptone, 0.5% yeast extract, and 2% agar, measured by the weight to volume ratio. The cultures were maintained at a temperature of 28 °C for a period of 15 days to ensure the conidia reached maturity [14].

### 2.2. Bioinformatic Analyses

All the protein sequences were sourced from the NCBI genome database, accessible at <https://www.ncbi.nlm.nih.gov/> (accessed on 25 December 2024). The specific nucleic acid sequence (MAC\_03189) and protein sequence (XP\_007809529.2) were obtained in FASTA format. Utilizing these protein sequences, a selection of diverse filamentous and non-filamentous fungi were made for BLASTp sequence alignment to identify similarities. Protein 3D structure maps were retrieved from the AlphaFold Protein Structure Database at <https://alphafold.ebi.ac.uk/> (accessed on 25 December 2024). For constructing the phylogenetic tree, MEGA v7.0 was employed with the neighbor-joining approach. The sequences

were aligned using the ClustalW algorithm integrated within MEGA and employing a bootstrap test with 1000 replicates. Another alignment parameter was set to default settings. The aligned sequences were then exported to GeneDoc 2.7 for homology analysis. Domain prediction was conducted using the SMART tool, available at <http://smart.embl.de/> (accessed on 25 December 2024), and TMH prediction was performed using TMHMM at <https://services.healthtech.dtu.dk/> (accessed on 25 December 2024). Additionally, BioXM v2.7.1 software was used to calculate the molecular weights and isoelectric points of the proteins.

### 2.3. Fungal Mutant Generation

The *MaNrtB* nucleic acid sequence (2535 bp) and an additional 2000 bp flanking the *MaNrtB* gene on both sides were obtained from the NCBI database. Among them, a 1.3 kb (left border) and a 1.4 kb (right border) flanking sequence of the *MaNrtB* gene locus were amplified using the primer pairs of *MaNrtB*-LF/*MaNrtB*-LR and *MaNrtB*-RF/*MaNrtB*-RR, respectively (Supplementary Table S1). The fragments were then successively ligated into the *Hind*III/*Xba*I and *Eco*RV/*Eco*RI-restricted pK2-PB vectors and verified by PCR using the primers LF/Pt-R and Bar-F/RR [15], respectively. Fungal transformation and validation of the transformants followed the methods described previously [16]. Potential  $\Delta$ *MaNrtB* mutants were identified on Czapek–Dox (CZA) medium supplemented with 500  $\mu$ g/mL glufosinate ammonium (Sigma, St. Louis, MO, USA), and the presence of the desired recombinant sequences was confirmed by PCR using the primer pairs of NrtB-VF/Pt-R and NrtB-VR/Bar-F. The pK2-sur vector was employed to generate the *MaNrtB* complemented strains (CPs). Initially, the full-length *eGFP* and *TtrpC* genes were cloned and ligated into the pK2-sur vector to create the pK2-eGFP-sur vector. Then, the promoter and ORF fragments were amplified from the WT genome using the primers NrtB-CP-F and NrtB-CP-R, and ligated to the *Hind*III/*Bam*HI-restricted pK2-eGFP-sur vector by one-step cloning to create the pK2-sur-*MaNrtB* construct [17], which was introduced into the  $\Delta$ *MaNrtB* strain. Candidate CP strains were selected on CZA medium with 20  $\mu$ g/mL chlorimuron ethyl (Sigma, Bellefonte, PA, USA), and recombinant events were verified by PCR using the primer pair of NrtB-CP-VF/GFP-VR. Reverse transcription quantitative PCR (RT-qPCR) analysis was performed to confirm the  $\Delta$ *MaNrtB* and CP strains. The schematic diagrams of the pK2-PB and pK2-sur vectors are shown in Figure S1. A complete list of the primers utilized in this study is provided in Table S1.

### 2.4. Conidial Germination and Conidial Yield Assays

Conidial suspensions at a concentration of  $1 \times 10^7$  conidia/mL were prepared with mature and freshly harvested conidia and a 0.05% Tween-80 solution. An aliquot of 50  $\mu$ L was uniformly spread onto 1/4 SDAY plates. Over a period of 10 h, at 2-h intervals, three 1 cm<sup>2</sup> sections were excised from each strain's plate. The number of germinated conidia was counted for every 100 conidia observed. Germination was defined as the emergence of a bud whose length was more than one-third of the width of the conidium. The germination rate was determined by the following formula: (number of germinated conidia/total number of conidia)  $\times$  100%. For assessing the conidial yield, 2  $\mu$ L of the conidial suspension ( $1 \times 10^6$  conidia/mL) was deposited into 24-well plates with 1 mL of 1/4 SDAY medium in each plate well. Every three days, the yield of conidia was measured. Briefly, the fungal cultures were transferred to a 2 mL centrifuge tube. After adding 1 mL of 0.05% Tween-80 solution for grinding, the mixture was vortexed. The suspension was then diluted, and the conidial concentration was determined using a hemocytometer. Each experiment was independently performed a minimum of three times to ensure reliability.

### 2.5. Stress Tolerance Assays

The 1/4 SDAY medium was amended with 0.5 M NaCl, 1 M sorbitol (SOR), 500 µg/mL Congo red (CR), 0.01% *w/v* sodium dodecyl sulfate (SDS), 50 µg/mL Calcofluor white (CFW), and 60 mmol/L H<sub>2</sub>O<sub>2</sub> to simulate adverse conditions. A 2 µL aliquot of conidial suspension ( $1 \times 10^6$  conidia/mL) from each strain was spread onto the modified culture plates and incubated at 28 °C for 6 days. The colony growth was then photographed and measured. To evaluate the heat-shock sensitivity of the fungal strains, the conidial suspensions ( $1 \times 10^7$  conidia/mL) were subjected to a water bath at 45 °C for durations of 2, 4, 6, and 8 h. Post-treatment, the suspensions were spread onto 1/4 SDAY medium and incubated at 28 °C for 20 h to determine the germination rates. For the UV-B tolerance of the fungal strains, the conidial suspensions ( $1 \times 10^7$  conidia/mL) were spread on 1/4 SDAY medium and exposed to UV-B radiation at a dose of 1350 mW/m<sup>2</sup> for periods of 0.5, 1.0, 1.5, and 2.0 h. Following exposure, the cultures were incubated at 28 °C for 20 h to assess the conidial germination. Each experiment was conducted in triplicate.

### 2.6. Bioassays

Two distinct bioassay methods were employed as previously described [15]. Briefly, in the topical inoculation approach, suspensions of the WT,  $\Delta MaNrtB$ , and CP strains, prepared in paraffin oil at a concentration of  $1 \times 10^7$  conidia/mL, were applied to the fifth-instar nymphs of locusts, *Locusta migratoria manilensis* (5 µL per nymph). For the intrahemocoel injection method, the conidia from the fungal strains were suspended in double-distilled water (ddH<sub>2</sub>O) at a concentration of  $1 \times 10^6$  conidia/mL and injected directly into the locust hemocoel (5 µL per nymph). For both inoculation techniques, each experimental group contained 20 fifth-instar nymphs, and the negative control groups were treated with pure paraffin oil and ddH<sub>2</sub>O, respectively. The survival rates of the locusts were monitored and documented at intervals of 12 h throughout the experiment.

To investigate the nutrient utilization efficiency of the various fungal strains, we employed liquid CZA medium along with two modified versions of CZA, SPM and TPM, to assess the fungal development under distinct nutritional conditions. The CZA medium was supplemented with 3% sucrose and 0.3% NaNO<sub>3</sub>, while the SPM contained 3% sucrose and 0.5% peptone, and the TPM was formulated with 3% trehalose and 0.5% peptone. Among the three media, CZA has nitrate as the main nitrogen source donor and thus can be used to assess the nitrate transport activity of NrtBp in *M. acridum*. TPM is used to mimic insect hemolymph, as described previously [18]. These media were designed to replicate and evaluate the growth of fungi in a variety of nutrient-rich environments. Briefly, a 30 µL sample of a conidial suspension at a concentration of  $10^7$  conidia/mL was introduced into each 30 mL medium, which was then incubated for 60 h at 28 °C with a shaker speed of 200 rpm to determine the biomass. This procedure was conducted in triplicate for each condition. To evaluate the host immune response, the total RNA was extracted from the fat bodies in the nymphs of locusts after injection to assess the expression levels of two key antimicrobial peptide (AMP) genes, *Attacin* and *Defensin*, using the protocol outlined in a previous study [19]. Each bioassay experiment was repeated three times.

### 2.7. Appressorium Formation Assays

Conidial suspensions for each strain were prepared in sterilized ddH<sub>2</sub>O to a density of  $1 \times 10^7$  conidia/mL. The sterilized locust hindwings were first coated with the conidial suspensions and then carefully spread onto pristine microscope slides for incubation at a controlled temperature of 28 °C. The conidia germination rate was monitored and recorded every two hours. Additionally, after a 12 h incubation period, the appressorium

formation rate was also counted. This experimental procedure was conducted in triplicate to ensure reliability.

To assess the fungal penetration capability, we placed sterilized locust hindwings on 1/4 SDAY plates. A 2  $\mu$ L aliquot of conidial suspension from each fungal strain, diluted to a concentration of  $1 \times 10^6$  conidia/mL, was dropped on the wings carefully. These were then incubated at 28 °C for 44 h. Following photography and documentation, the wings were removed to allow continued incubation for an additional four days, with photographs taken to document the colony morphology. As a control, conidial suspensions were also directly inoculated onto 1/4 SDAY medium and incubated at 28 °C for a duration of 6 days. Each treatment contained 10 wings and these assays were repeated three times.

### 2.8. Data Analyses

A one-way ANOVA test was conducted to evaluate the phenotypic estimates, followed by Tukey's honestly significant difference (HSD) test to ascertain the significance of any observed differences among the groups.

## 3. Results

### 3.1. Features of *MaNrtB* and Mutant Generation

Bioinformatics analysis revealed that there is only one putative Nrt gene, designated as *MaNrtB*, in *M. acridum*. The *MaNrtB* gene spans 1612 base pairs and encodes a protein of 502 amino acids, distributed across two exons. The calculated molecular weight for the *MaNrtB* protein is 53.75 kDa, with an isoelectric point of 7.8. Domain analysis, conducted via the SMART online tool, indicated the presence of an MFS domain. As with other reported Nrt homologues [6,11,12,20–22], the tertiary structure of NrtB in *M. acridum* putatively contains 12 transmembrane-spanning alpha helices (TMHs) that are colored in blue with a less conserved intracellular central loop (Figures 1A and S2). The sequence alignment of the orthologous NrtB proteins revealed that these TMH domains are highly conserved, whereas the central loop region exhibits a lack of order (Figure S3). Additionally, phylogenetic analysis grouped *MaNrtB* together with several of its homologs that have been evidenced to possess nitrate transport capacity, such as *A. nidulans* [6] and *F. oxysporum* [11] (Figure 1B), and these domains are notably conserved in filamentous fungi and exhibit lower conservation in yeast (Figure 1B). Overall, the significant similarity in the tertiary structures of these proteins suggests that they likely have similar functions. *MaNrtB*-knockout transformants were generated through homologous recombination. The CP strain was derived using the ectopic strategy (Figure 2B). The  $\Delta$ *MaNrtB* and CP strains were validated by PCR (Figure S4). Furthermore, the expression levels of the *MaNrtB* gene in the WT,  $\Delta$ *MaNrtB*, and CP strains were quantified using RT-qPCR. The expression levels of *MaNrtB* in the WT and CP strains were markedly higher than in the  $\Delta$ *MaNrtB* strain, confirming the successful generation of both the  $\Delta$ *MaNrtB* and CP strains (Figure 2C).

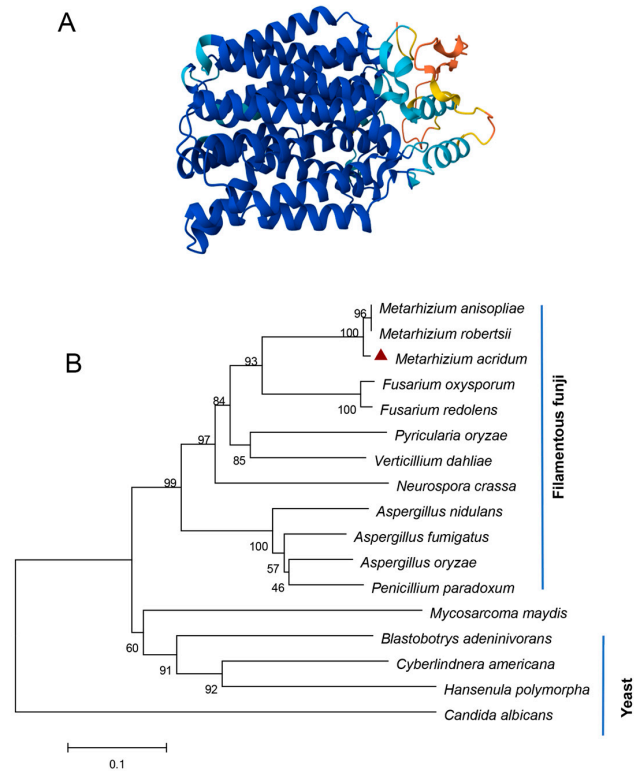


**Figure 1.** Bioinformatics of *MaNrtB*. **(A)** Domain analysis of *MaNrtB*, which contains 12 transmembrane (TM) spanning alpha helices marked in a blue color. **(B)** A phylogenetic tree was constructed with the *NrtB* protein sequences of *Metarhizium acridum* (EFY90826.1), *Metarhizium anisopliae* (KAF5125400.1), *Metarhizium robertsii* (XP\_007820472.2), *Fusarium oxysporum* (XP\_018232784.1), *Fusarium redolens* (XP\_046056618.1), *Pyricularia oryzae* (XP\_003710887.1), *Verticillium dahlia* (KAF3360447.1), *Neurospora crassa* (XP\_957430.2), *Aspergillus nidulans* (XP\_658612.1), *Aspergillus fumigatus* (KAH1494629.1), *Aspergillus oryzae* (EIT78908.1), *Penicillium paradoxum* (XP\_057035394.1), *Mycosarcoma maydis* (XP\_011390345.1), *Blastobotrys adeninivorans* (CAQ77149.1), *Cyberlindnera americana* (QFR37177.1), *Hansenula polymorpha* (XP\_018213600.1), and *Candida albicans* (XP\_717110.1). The red triangle represents the *NrtB* homologous protein in *M. acridum*.

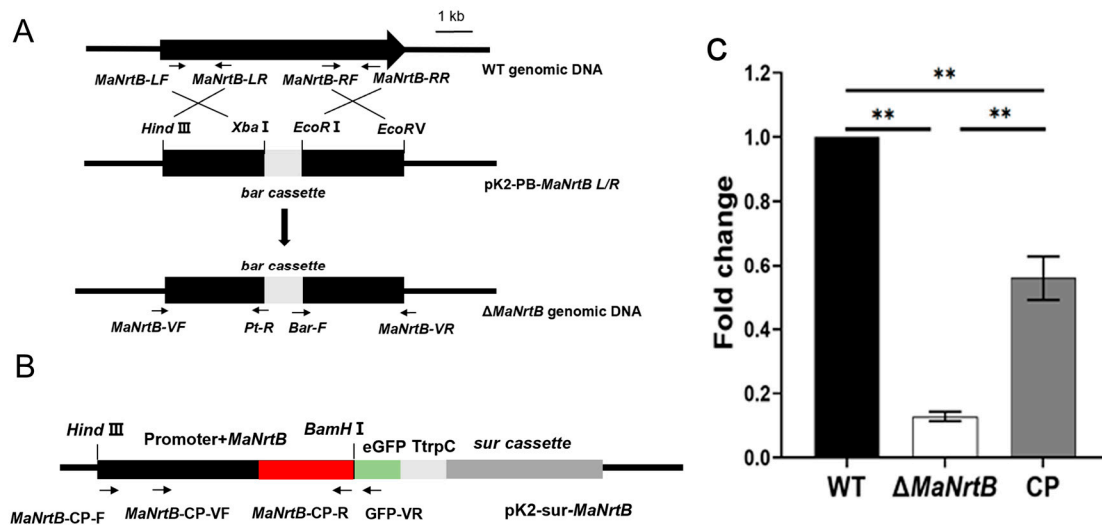


**Figure 2.** Disruption and complementation of *MaNrtB*. **(A,B)** Schematic diagrams of the knockout and complementation vector constructions. Black arrows indicate the positions of the primers. **(C)** Verification of transformants by RT-qPCR. Error bars = mean  $\pm$  SEM. Asterisks indicate a significant difference at **(\*\*)**  $p < 0.01$ .

### 3.2. Disruption of *MaNrtB* Impaired Conidial Germination but Not Conidial Yield

Our initial assessment focused on the germination rates and conidial yields of the different fungal strains. It was observed that the  $\Delta MaNrtB$  strain exhibited a considerably reduced germination rate compared to both the WT and CP strains after 4 h of incubation (Figure 3A). Furthermore, the  $\Delta MaNrtB$  strain required a significantly longer time to reach 50% germination ( $GT_{50}$ ) (Figure 3B). In contrast, the conidial yield among the three strains was found to be statistically indistinguishable (Figure 3C). Collectively, these findings suggest that the disruption of the *MaNrtB* gene in *M. acridum* led to the retardation of conidial germination without impacting the conidial production.

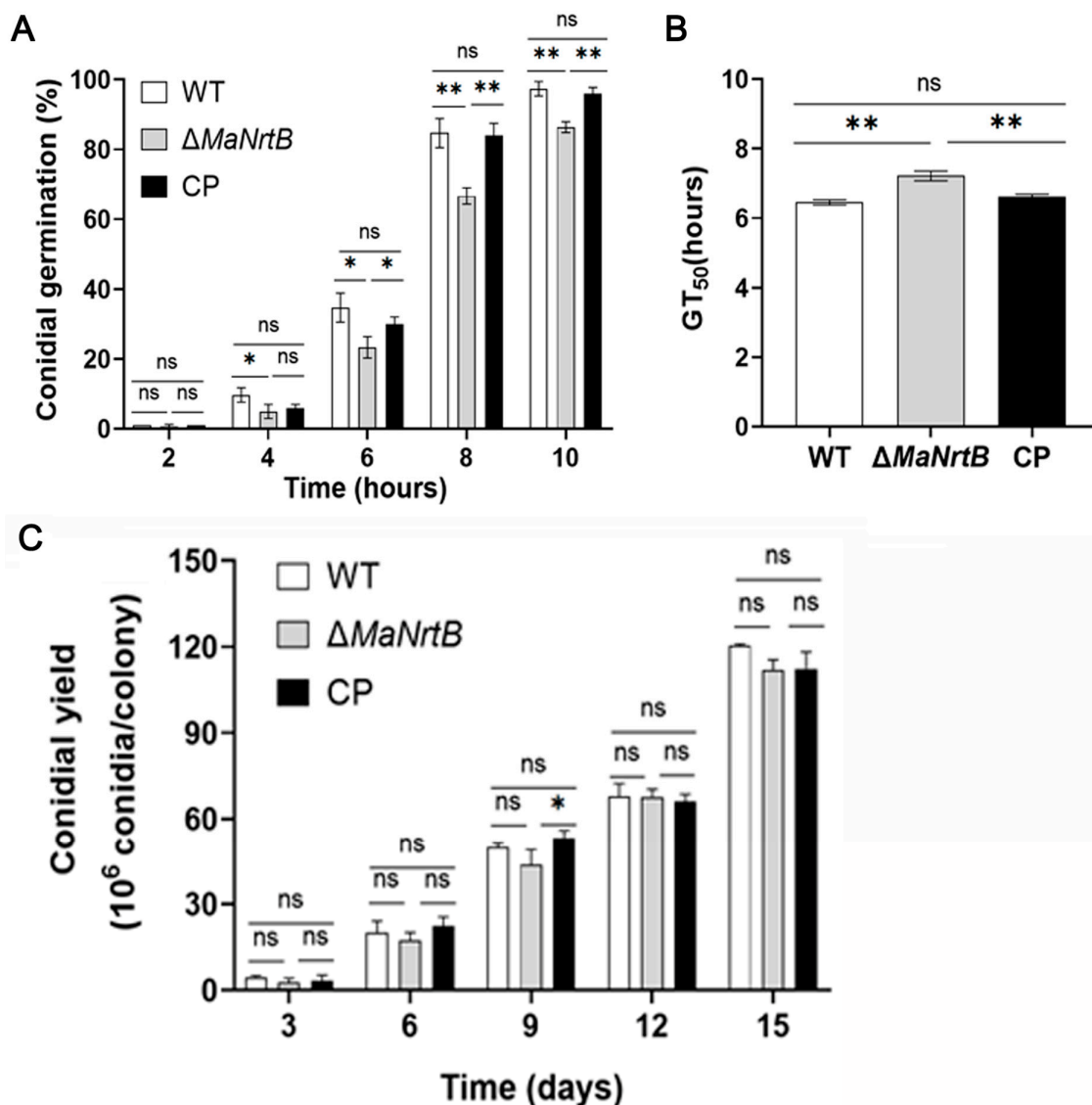


**Figure 3.** Deletion of *MaNrtB* affected the conidial germination but not the conidial yield. (A) The germination rate of each strain of *M. acridum* at different times. (B) The  $GT_{50}$  of each strain during germination. (C) The conidia yield of each strain on 1/4 SDAY medium for 3 d, 6 d, 9 d, 12 d, and 15 d. Error bars = mean  $\pm$  SEM. Asterisks indicate a significant difference at (\*)  $p < 0.05$ , (\*\*)  $p < 0.01$ , or (ns)  $p > 0.05$ .

### 3.3. Disruption of *MaNrtB* Affected Fungal Stress Tolerances

The ability to withstand environmental stress is crucial for EPF. Thus, we examined the UV-B and heat-shock stress tolerances of the WT,  $\Delta MaNrtB$ , and CP strains. Post-UV-B irradiation, the  $\Delta MaNrtB$  strain exhibited a markedly reduced conidial germination rate after

one hour and a significantly lower  $GT_{50}$  compared to the WT and CP strains (Figure 4A,B). Conversely, under heat-shock conditions, the  $\Delta MaNrtB$  strain displayed a higher germination rate after four hours of treatment, with a notably elevated  $GT_{50}$  (Figure 4C,D). These findings suggest that the disruption of *MaNrtB* in *M. acridum* compromised its UV-B resistance but enhanced its heat tolerance. Furthermore, spot assays revealed that the  $\Delta MaNrtB$  strain formed smaller colonies relative to the WT and CP strains on 1/4 SDAY medium supplemented with SOR, NaCl, H<sub>2</sub>O<sub>2</sub>, CR, and CFW (Figure 5), indicating that the  $\Delta MaNrtB$  strain was more susceptible to hyperosmotic, oxidative, and cell wall stresses.

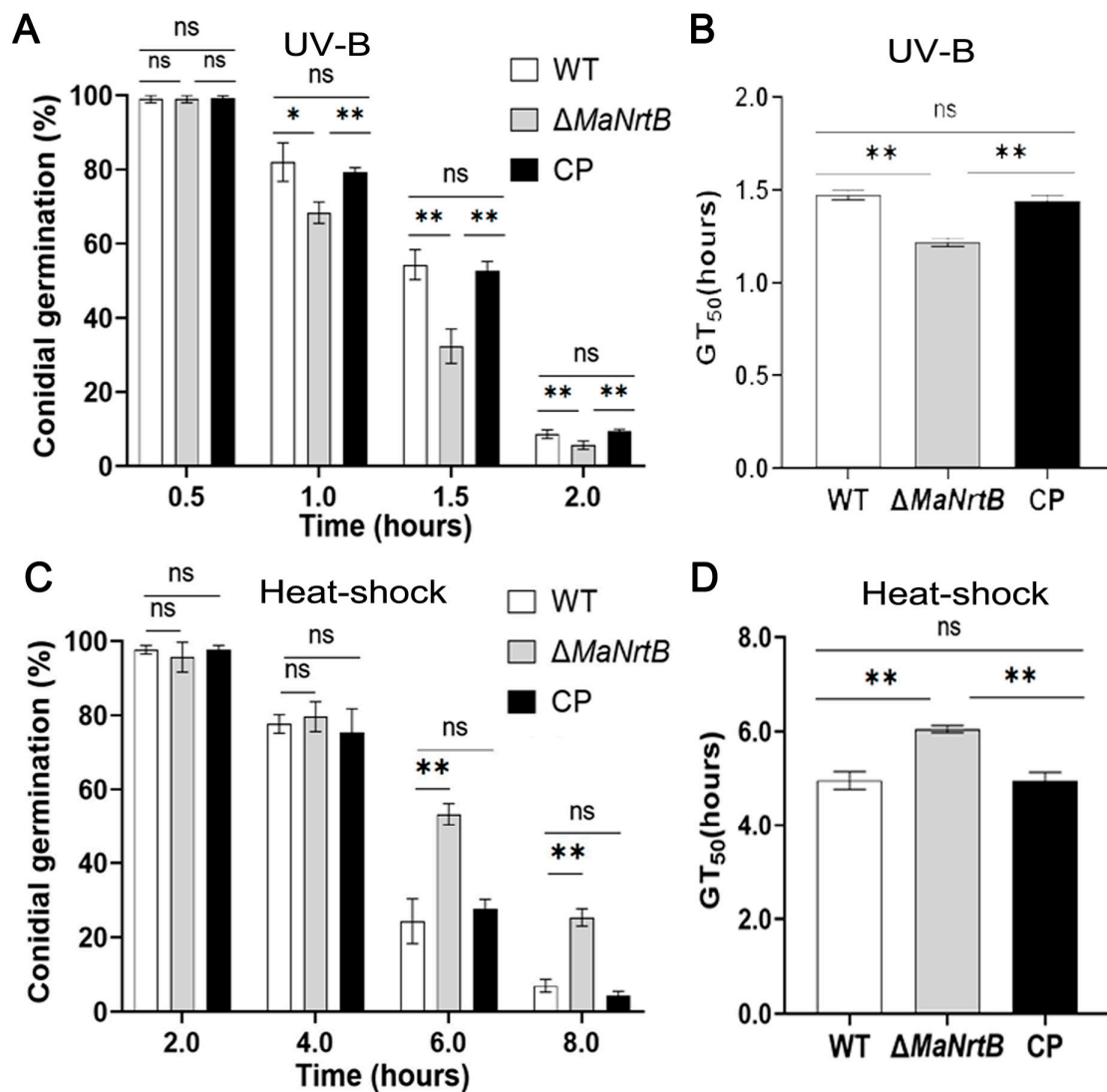


**Figure 4.** Deletion of *MaNrtB* reduced the fungal tolerance to UV-B irradiation but increased the fungal tolerance to heat shock. (A) Conidial germination treated with UV-B irradiation for 0.5 h, 1.0 h, 1.5 h, and 2.0 h. (B) The  $GT_{50}$  under UV-B irradiation. (C) Germination rates treated with heat shock for 2.0 h, 4.0 h, 6.0 h, and 8.0 h. (D)  $GT_{50}$  under heat shock. Error bars = mean  $\pm$  SEM. Asterisks indicate a significant difference at (\*)  $p < 0.05$ , (\*\*)  $p < 0.01$ , or (ns)  $p > 0.05$ .

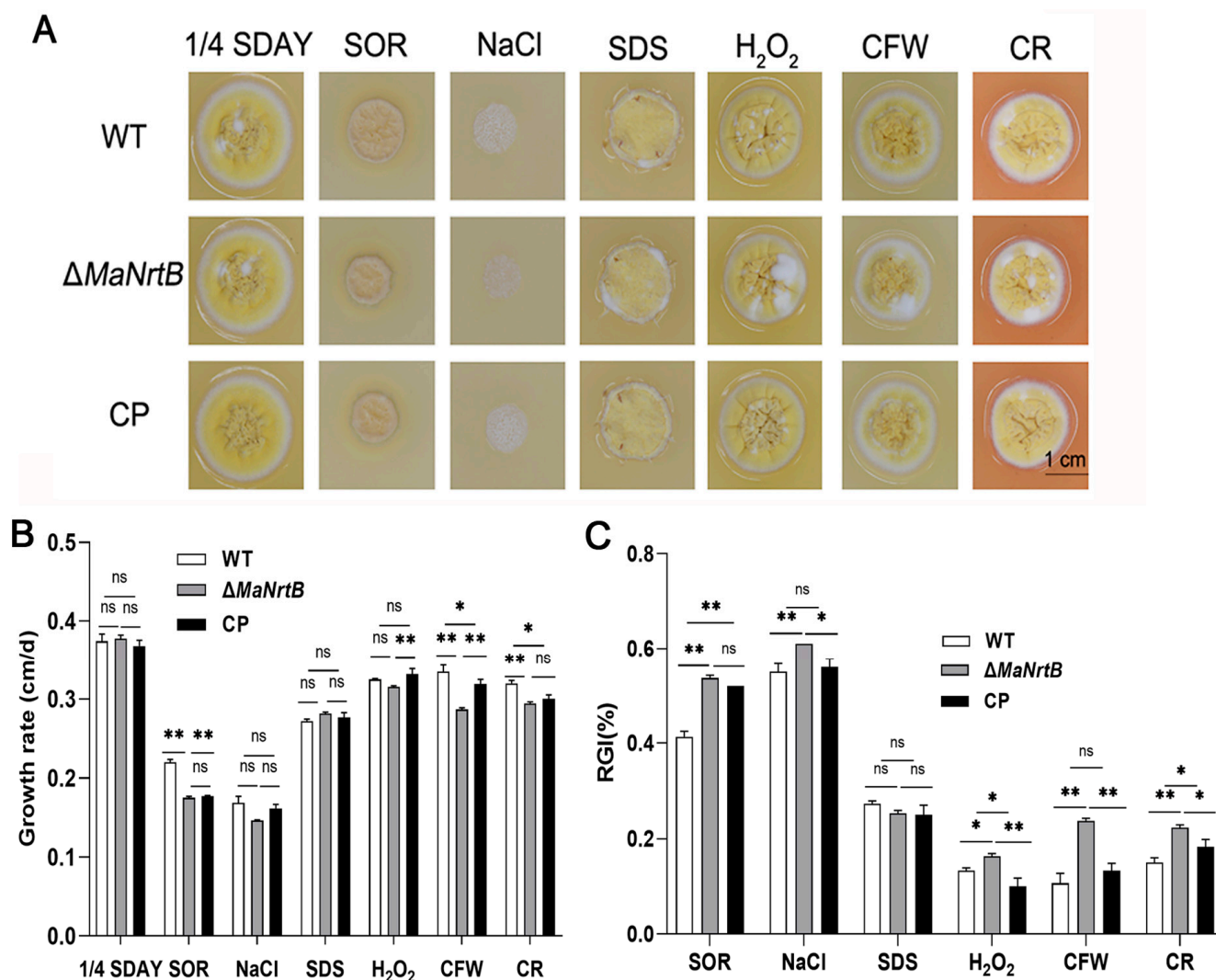


**Figure 5.** Disruption of *MaNrtB* reduced tolerances to multiple chemical reagents. (A) Colony morphologies of *M. acridum* strains grown for 6 days on 1/4 SDAY with different chemical reagents. (B) The growth rates of *M. acridum* strains under different chemical reagents. (C) Relative growth inhibition rates of *M. acridum* strains under different chemical reagents. Error bars = mean  $\pm$  SEM. Asterisks indicate a significant difference at (\*)  $p < 0.05$ , (\*\*)  $p < 0.01$ , or (ns)  $p > 0.05$ .

### 3.4. Disruption of *MaNrtB* Attenuated Fungal Virulence

To assess the role of *MaNrtB* in virulence, we conducted bioassays using two infection methods, topical application and direct intrahemocoel injection. With topical application of the WT or CP strains, all the locusts succumbed by 8.5 days post-inoculation (dpi), whereas those inoculated with the  $\Delta$ *MaNrtB* strain died after 10.0 dpi (Figure 6A). The median lethal time (LT<sub>50</sub>) for the  $\Delta$ *MaNrtB* strain was  $6.26 \pm 0.80$  days, which was significantly longer than the  $4.90 \pm 0.69$  days for the WT and  $5.32 \pm 0.73$  days for the CP strain ( $p < 0.05$ ; Figure 6B). Similarly, when using the intrahemocoel injection method, the survival rates of the locusts infected with the  $\Delta$ *MaNrtB* strain were also significantly higher than those infected with the WT or CP strains (Figure 6C). Likewise, the LT<sub>50</sub> for the  $\Delta$ *MaNrtB* strain, at  $4.64 \pm 0.67$  days, was significantly longer than the  $3.55 \pm 0.56$  days for the WT and  $3.97 \pm 0.60$  days for the CP strains ( $p < 0.05$ ; Figure 6D). Collectively, these findings indicate that *MaNrtB* plays a significant role in the virulence of *M. acridum*.

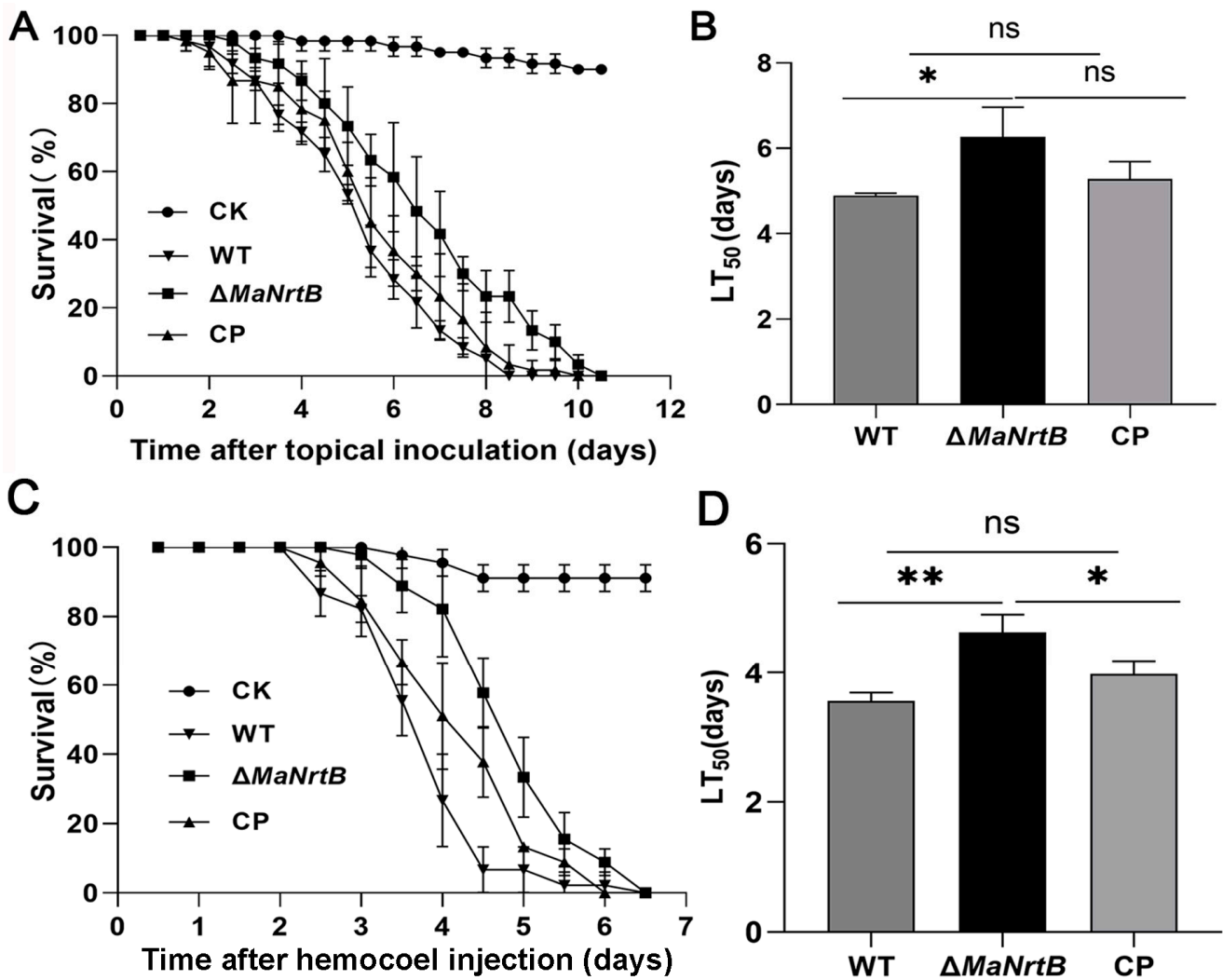


**Figure 6.** Disruption of *MaNrtB* impaired fungal virulence. (A) Survival rates of locusts after topical application of fungal conidia. Liquid paraffin oil as a control. (B) LT<sub>50</sub> of fungal strains against locusts by topical application. (C) Survival rates of locusts after hemocoel injection of conidia. Sterile water as a control. (D) LT<sub>50</sub> of fungal strains against locusts by hemocoel injection. Error bars = mean ± SEM. Asterisks indicate a significant difference at (\*)  $p < 0.05$ , (\*\*)  $p < 0.01$ , or (ns)  $p > 0.05$ .

To explore whether the *MaNrtB* deletion impacts fungal penetration, we inoculated *M. acridum* on the hind wings of locusts and analyzed the penetration ability of each strain. The results showed that compared to the WT and CP, the  $\Delta MaNrtB$  strain formed the smallest colony with the lowest penetration ability (Figure 7A). To elucidate the functions of *MaNrtB* in the infectious process, we analyzed the germination of conidia and the formation of appressoria on the locust hind wings for the WT,  $\Delta MaNrtB$ , and CP strains. The absence of *MaNrtB* led to slower conidial germination on the locust hind wings (Figure 7B,C). Microscopic observation showed that all three strains formed normal appressorium, but the *MaNrtB* mutation also resulted in significantly decreased appressorium formation ( $p < 0.01$ ; Figures S5 and 7D). After a 24 h induction on locust wings, the  $\Delta MaNrtB$  strain formed about 30% normal appressoria, in contrast to the over 50% observed in both the WT and CP strains (Figure 7D).

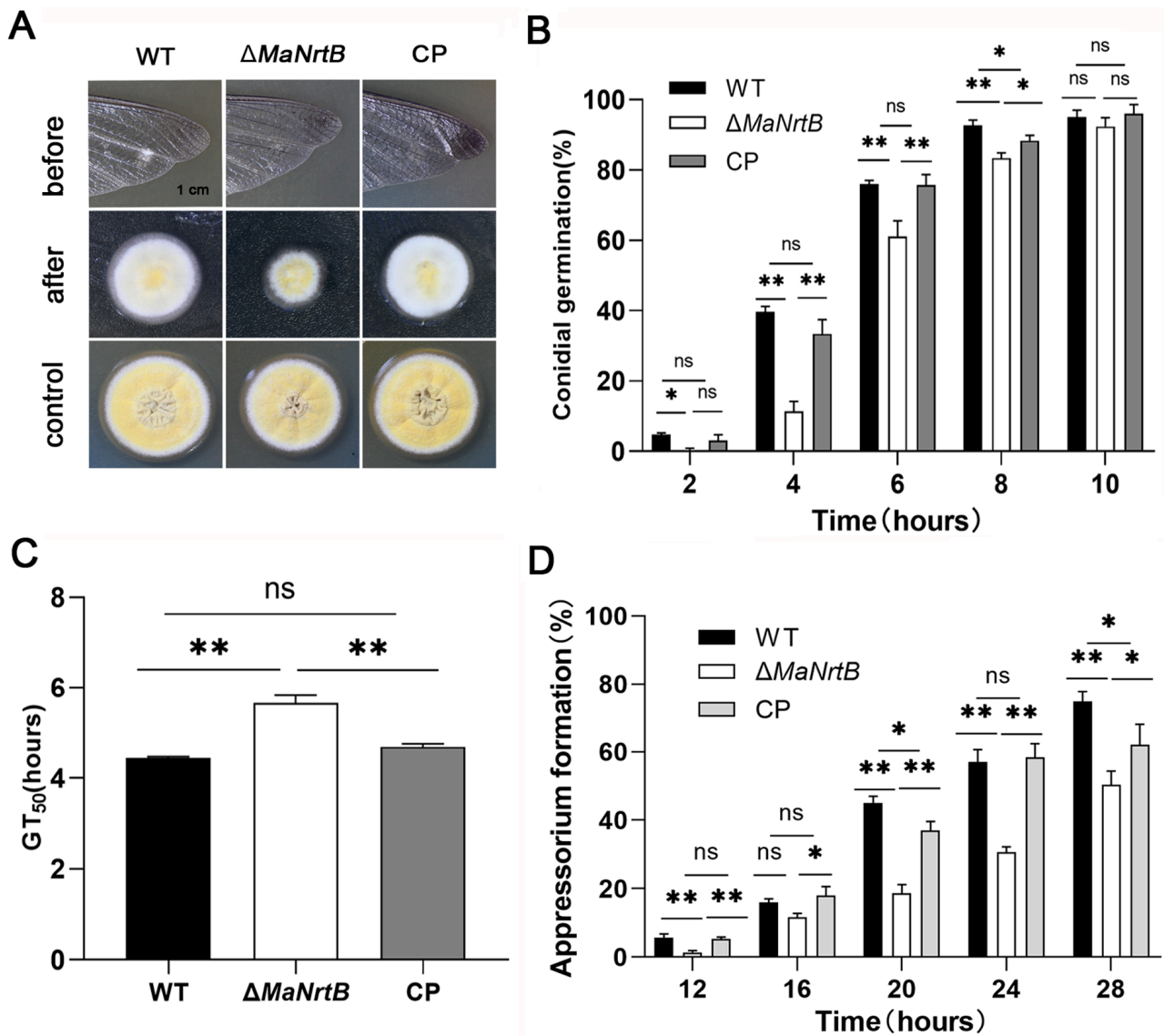


**Figure 7.** Disruption of *MaNrtB* affected locust cuticle penetration of *M. acridum*. (A) Penetration assays. (B) The germination rate of the WT,  $\Delta MaNrtB$  and CP strains growing on the hind wings of locust for 2 h, 4 h, 6 h, 8 h and 10 h. (C) The GT<sub>50</sub> of each strain on the hind wings of locust. (D) The appressorium formation rates of the WT,  $\Delta MaNrtB$  and CP strains growing on the hind wings of locust for 12 h, 16 h, 20 h, 24 h, and 28 h. Error bars = mean  $\pm$  SEM. Asterisks indicate a significant difference at (\*)  $p < 0.05$ , (\*\*)  $p < 0.01$ , or (ns)  $p > 0.05$ .

To verify whether the *MaNrtB* deletion impacts fungal colonization in hemolymph, we first simulated fungal growth in different media, then quantified the biomass, and analyzed the uptake of carbon and nitrogen sources. It was found that the fungi accumulated the most biomass in SPM medium containing sucrose and peptone, which were the preferable choice for both nitrogen and carbon sources, and the  $\Delta MaNrtB$  mutant accumulated about 22% biomass less than the WT (Figure 8A). Replacing sucrose with trehalose widened the gap to about 43% in TPM (Figure 8A). In the nutrient-poor CZA standard medium, the gap in accumulated biomass reached 56% (Figure 8A). Furthermore, to probe whether the *MaNrtB* gene contributed to the ability of the fungus to evade host immune defenses, the expression levels of *Defensin* and *Attacin*, Toll- and/or Imd-activating antimicrobial peptide genes involved in fungal recognition and immune response in the insect fat bodies were analyzed after injection with conidial suspension from different fungal strains. The results displayed that lower levels of expression of *Attacin* (32%) and *Defensin* (43%) were found

in the locusts infected by the *MaNrtB* strain compared to those infected by the WT after 24 dpi (Figure 8B).

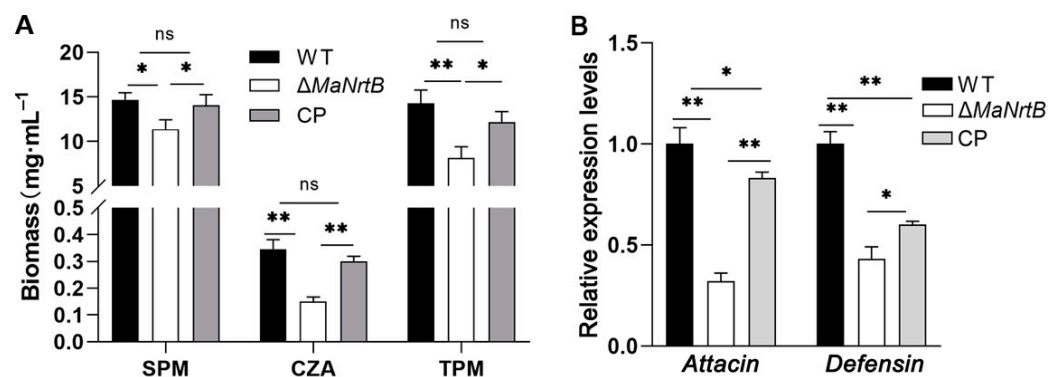


**Figure 8.** Disruption of *MaNrtB* impaired fungal growth in locust hemolymph. (A) The biomass levels were quantified from the 3-day-old submerged cultures in CZA and three amended media, sucrose–peptone medium (SPM) and trehalose–peptone medium (TPM). (B) The relative expression of *Attacin* and *Defensin* in locust fat bodies was determined at 24 h after injection by RT-qPCR. Error bars = mean  $\pm$  SEM. Asterisks indicate a significant difference at (\*)  $p < 0.05$ , (\*\*)  $p < 0.01$ , or (ns)  $p > 0.05$ .

#### 4. Discussion

NrtB, a conserved nitrate transporter in filamentous fungi, has been the subject of limited research regarding its molecular mechanisms and their relation to fungal growth. In our study, we employed homologous recombination to generate *MaNrtB* deletion and complementation transformants, conducting a thorough analysis of the *MaNrtB* functions. Our results indicated that *MaNrtB*, the nitrate transporter gene, plays important roles in the conidial germination, stress tolerances, and virulence of the entomopathogenic fungus *M. acridum*. These findings provide new perspectives for understanding the biological properties and pathogenesis of EPF.

Nitrogen sources play a pivotal role in the morphological development, production of secondary metabolites, and virulence of EPF [23]. Typically, fungi prioritize certain nitrogen sources, such as ammonium, and repress the assimilation of others, such as nitrate, a phenomenon termed nitrogen catabolite repression (NCR) [24]. In Ascomycetes, including *A. nidulans*, the key regulators AreA and AreB govern nitrogen metabolism, with nitrate metabolism gene activation primarily under the control of the transcription factors AreA and NirA [25–27]. AreA acts as a positive regulator that can alleviate NCR, while NirA is a transcription factor specific to the nitrate assimilation pathway, induced by nitrate or nitrite [28]. NmrA is another central regulator within the NCR pathway, modulating fungal nitrogen metabolism by interacting with and suppressing the activity of AreA and AreB [29–32]. In our previous research, we established a library of differentially expressed genes responsive to nitrate [33]. Among the genes, *MaNCP1*, a C2H2-type transcription factor gene, was identified to modulate nitrate metabolism by interacting with the *MaNmrA* in *M. acridum* [34,35]. *MaNCP1* influences nitrate metabolism and impacts nitric oxide (NO) synthesis [34], which can engage in various signal transduction pathways, leading to phenotypic alterations in the fungus [36]. Nitrate can trigger the upregulation of *MaNCP1* and *MaNmrA*, and the expression of the nitrate transporter gene *MaNrtB* is downregulated following the deletion of *MaNCP1* or *MaNmrA* [34]. This suggests reduced transport of nitrate from the extracellular environment into the cell, yet the nitrate content in the  $\Delta MaNCP1$  and  $\Delta MaNmrA$  strains was significantly higher than in the wild-type strain, indicating a severe disruption in nitrate catabolism [34]. As a key component of the conserved nitrate assimilation pathway, Nrts regulate cellular nitrogen utilization and

further influence fungal growth and development [37]. In our research, the  $\Delta MaNrtB$  strain displayed slower growth, reduced stress resistance, and decreased virulence against locusts, just like the mutant of  $\Delta MaNCP1$  [38] and  $\Delta MaNmrA$  strains [39], underscoring the important role of nitrate metabolism in sustaining fungal growth.

The capacity of conidia to withstand environmental stress is critical for the efficacy of EPF in the field, underscoring the importance of identifying robust strains for practical applications [40]. Our research revealed that the  $\Delta MaNrtB$  strain showed reduced tolerances to UV-B and cell wall stress but enhanced resistance to heat shock. The fungal cell wall is the primary defense against external stressors [41]. Compounds such as CFW and CR are commonly utilized to challenge fungal cell walls in vitro [42]. CFW interferes with chitin assembly, and CR inhibits  $\beta$ -glucan synthesis, both leading to cell wall damage and triggering cell wall stress responses [43]. In *Arabidopsis thaliana*, a co-expression analysis of cell wall remodeling genes with nitrate and ammonium transporters revealed that there is a notably strong correlation between the regulation of cell wall remodeling and nitrate assimilation processes, while ammonium transporters appeared to have a more limited role in these co-expression networks [44]. Thus, the inhibited growth of  $\Delta MaNrtB$  on 1/4 SDAY medium containing CR and CFW suggests that *MaNrtB* also plays a role in maintaining cell wall integrity.

The conidial germination rate of the  $\Delta MaNrtB$  strain was diminished, echoing observations in *U. maydis* [12] and *F. oxysporum* [11]. However, the production of conidia remained unaffected in the  $\Delta MaNrtB$  strain, suggesting that the *MaNrtB* gene is pivotal for conidial germination but exerts minimal influence on the process of conidiation. In *F. fujikuroi*, a reduction in biomass was noted in mutants of the nitrate transporter protein compared to the wild type [45]. Consistent with prior fungal studies, the growth rate of *F. graminearum* is dependent on the availability and type of nitrogen sources [46]. In *B. bassiana*, deprivation of nitrogen nutrients leads to reduced conidium production [47]. Disrupting the gene encoding the nitrate-responsive transcription factor NirA in *B. bassiana* causes reduced growth rates and diminished efficiency in utilizing nitrate and urea [48]. This supports the notion that the highly conserved nitrate assimilation pathway is crucial for promoting growth across various filamentous fungi.

Elucidating the impact of nitrogen sources on fungal virulence is helpful in developing novel pest control strategies. A successful infection hinges on the ability of a pathogen to overcome host defenses and secure vital nutrients necessary to complete its life cycle [49]. The nitrate assimilation pathway plays a significant role in fungal virulence. In *Colletotrichum acutatum*, a strain with a deletion of the *NirA1* gene could not grow on media using nitrate or nitrite as the sole nitrogen source and displayed reduced virulence on strawberry leaves [50]. In *N. crassa*, growth tests with nitrate as the sole nitrogen source showed that the homologous protein *nit-10* mutant was unable to grow with a low nitrate concentration [51]. In the plant pathogen *Magnaporthe oryzae*, the trehalose-6-phosphate synthase enzyme (Tps1) links glucose-6-phosphate metabolism to nitrogen source utilization, modulating nitrate reductase activity [52]. Moreover, a study showed that there is a genetic switch that consists of Tps1 and the nitrogen metabolite repressor gene *NMR1* [53]. This genetic switch controls the expression of certain nitrogen-utilization GATA-factor transcriptional factors downstream, including ASD4 (the homologous protein to AreB in *M. oryzae*), and it is necessary for regulation of a set of genes that are expressed during appressorium-mediated infection in *M. oryzae* [53]. Further research has reported that targeted deletion of *Asd4* led to an increase in glutamine levels in *M. oryzae*, which can further activate the TOR pathway and promote autophagy, thereby promoting hyphal growth while impeding appressorium formation [54,55]. The phenotypic observations of the  $\Delta MaAreB$  strain [55] were consistent with the *M. oryzae* *ASD4* mutant [56]. In our

study, the disruption of the *MaNrtB* gene led to delayed conidial germination, reduced appressorium formation, and attenuated growth within the insect host; thus, we speculate that the disorder of the nitrate assimilation pathways may have led to changes in the glutamine levels in vivo and influenced the TOR pathway, ultimately resulting in impaired growth and virulence in *M. acridum*.

For entomopathogenic fungi, the capacity to penetrate the insect cuticle and proliferate in the hemolymph is crucial for fungal virulence [57]. Fungi not only need to overcome the host immune response but also compete for nutrients with other microorganisms within the host; for instance, *M. rileyi* generates compounds that inhibit the proliferation of competing microorganisms, thereby facilitating its own swift expansion and contributing to the demise of the host [58]. In our study, media containing different carbon and nitrogen sources were used to simulate the growth pattern of fungi facing different nutrient environments. Correspondingly, the  $\Delta MaNrtB$  strain showed significantly decreased total biomass in each media compared to the WT and CP strains, suggesting that the deletion of *MaNrtB* contributes to trehalose utilization, which would further affect fungal growth and dimorphic transformation within the host haemocoel, and hence fungal virulence [56]. In the nutrient-poor CZA standard medium, the gap in accumulated biomass reached 56%, while the absence of Nrts greatly limited fungal growth in nitrate-containing environments, which is consistent with previous studies [7,10–12]. Furthermore, fungal cells must overcome the host immune activity to propagate by yeast-like budding in the host haemocoel [59]. We assessed the immune response of locusts by quantifying the expression levels of two AMP genes, *Attacin* and *Defensin*. In this study, the locusts infected by  $\Delta MaNrtB$  displayed decreased AMP gene expression, implicating an impaired ability of the  $\Delta MaNrtB$  mutant in the fungal evasion from locust immunity defense. Given that the mutant strain exhibits a reduced growth rate in media with varying nutrient compositions, this could potentially impair its development under diverse conditions. Such developmental constraints might, in turn, account for the insect's diminished defensive response.

In summary, our study sheds light on the multifaceted functions of the *NrtB* gene in the entomopathogenic fungus *M. acridum*. We have demonstrated that *NrtB* plays a pivotal role in multi-stress tolerance, nutrient assimilation, and fungal pathogenicity. These insights contribute to a deeper understanding of the molecular mechanisms underlying fungal virulence.

**Supplementary Materials:** The following supporting information can be downloaded at <https://www.mdpi.com/article/10.3390/jof11020111/s1>, Figure S1: The schematic diagrams of the pK2-PB and pK2-sur vectors. (A) *Hind*III/*Xba*I and *Eco*RV/*Eco*RI-restricted pK2-PB vectors used to insert the left border and right border of *MaNrtB*, respectively. Pt-R and Bar-F are universal primers located in the *bar* cassette. (B) The eGFP and TtrpC sequences were enzymatically ligated to the 5' end of the sur cassette, resulting in the formation of the PK2-eGFP-SUR vector. This construct can be used for the construction of any gene C-terminal fusion EGFP vector. Figure S2: Structure prediction of the *MaNrtB* protein. (A) Comparison of the three-dimensional structure of the nitrate transporter protein Nrt in different organisms. The three-dimensional structures of these Nrt homologous proteins are similar. Accession ID: *Aspergillus nidulans* CrnA (XP\_658612.1), *A. nidulans* NrtB (AAL50818.1), *N. crassa* Nit-10 (XP\_957430.2), *M. maydis* Nrt (XP\_011390345.1), *H. polymorpha* (XP\_018213600.1), *A. thaliana* NRT 2.1 (NP\_172288.1), and *Escherichia coli* (CAD6015891.1). (B) Transmembrane structure analysis of the *MaNrtB* protein. The 12 transmembrane domains are highlighted with a red color. Figure S3: Alignments of the amino acid sequences of the *NrtB* protein with those in other fungi. The MFS structural domain is marked by a red line. The transmembrane domain is marked by a black line. Accession numbers are as follows: *M. acridum* (XP\_007809529.2), *M. anisopliae* (KAF5125400.1), *M. robertsii* (XP\_007820472.2), *A. fumigatus* (KAH1494629.1), *F. redolens* (XP\_046056618.1), *N. crassa* (XP\_957430.2), *P. oryzae* (XP\_003710887.1), *P. paradoxum* (XP\_057035394.1).

and *V. dahliae* (KAF3360447.1). Figure S4: Validations of the  $\Delta MaNrtB$  and CP strains by PCR using the primer pairs of NrtB-VF/Pt-R (A), Bar-F/NrtB-VR (B), NrtB-CP-VF/GFP-VR (C), and TEF-F/TEF-R (D). Figure S5: Photomicrographs of the appressoria formed by WT,  $\Delta MaNrtB$ , and CP. All three strains were able to form normal appressoria, but there were no obvious differences in their morphology. Table S1: Primers used in this study. Table S2: Data of the fungal biomass measurements in different media.

**Author Contributions:** Conceptualization, Y.X. and K.J.; methodology, Y.X. and K.J.; software, J.W.; validation, K.J.; formal analysis, J.W. and K.J.; investigation, J.W. and Y.Z.; resources, Y.X. and K.J.; data curation, J.W. and Y.Z.; writing—original draft preparation, J.W. and K.J.; writing—review and editing, K.J.; visualization, J.W.; supervision, Y.X. and K.J.; project administration, Y.X. and K.J.; funding acquisition, Y.X. and K.J. All authors have read and agreed to the published version of the manuscript.

**Funding:** This research was funded by the National Natural Science Foundation of China (32172479), the Natural Science Foundation Project of Chongqing (CSTB2022NSCQ-MSX1185), the technology innovation and application development project of Chongqing (CSTB2023TIAD-KPX0045), and the fundamental research funds for the central universities (2024CDJXY016).

**Institutional Review Board Statement:** Not applicable.

**Informed Consent Statement:** Not applicable.

**Data Availability Statement:** Data are contained within the article and Supplementary Materials.

**Conflicts of Interest:** The authors declare no conflicts of interest.

## References

- Savary, S.; Willocquet, L.; Pethybridge, S.J.; Esker, P.; McRoberts, N.; Nelson, A. The global burden of pathogens and pests on major food crops. *Nat. Ecol. Evol.* **2019**, *3*, 430–439. [[CrossRef](#)] [[PubMed](#)]
- Butt, T.M.; Coates, C.J.; Dubovskiy, I.M.; Ratcliffe, N.A. Entomopathogenic fungi: New insights into host-pathogen interactions. *Adv. Genet.* **2016**, *94*, 307–364. [[PubMed](#)]
- Thomas, M.B.; Read, A.F. Can fungal biopesticides control malaria? *Nat. Rev. Microbiol.* **2007**, *5*, 377–383. [[CrossRef](#)] [[PubMed](#)]
- Morschhäuser, J. Nitrogen regulation of morphogenesis and protease secretion in *Candida albicans*. *Int. J. Med. Microbiol.* **2011**, *301*, 390–394. [[CrossRef](#)]
- Magasanik, B.; Kaiser, C.A. Nitrogen regulation in *Saccharomyces cerevisiae*. *Gene* **2002**, *290*, 1–18. [[CrossRef](#)]
- Unkles, S.E.; Hawker, K.L.; Grieve, C.; Campbell, E.I.; Montague, P.; Kinghorn, J.R. *crnA* encodes a nitrate transporter in *Aspergillus nidulans*. *Proc. Natl. Acad. Sci. USA* **1991**, *88*, 204–208. [[CrossRef](#)]
- Zhou, J.J.; Trueman, L.J.; Boorer, K.J.; Theodoulou, F.L.; Forde, B.G.; Miller, A.J. A high affinity fungal nitrate carrier with two transport mechanisms. *J. Biol. Chem.* **2000**, *275*, 39894–39899. [[CrossRef](#)] [[PubMed](#)]
- Pellizzaro, A.; Alibert, B.; Planchet, E.; Limami, A.M.; Morère-Le Paven, M.C. Nitrate transporters: An overview in legumes. *Planta* **2017**, *246*, 585–595. [[CrossRef](#)]
- Akhtar, N.; Karabika, E.; Kinghorn, J.R.; Glass, A.D.; Unkles, S.E.; Rouch, D.A. High-affinity nitrate/nitrite transporters NrtA and NrtB of *Aspergillus nidulans* exhibit high specificity and different inhibitor sensitivity. *Microbiology* **2015**, *161*, 1435–1446. [[CrossRef](#)]
- Machín, F.; Medina, B.; Navarro, F.J.; Pérez, M.D.; Veenhuis, M.; Tejera, P.; Lorenzo, H.; Lancha, A.; Siverio, J.M. The role of Ynt1 in nitrate and nitrite transport in the yeast *Hansenula polymorpha*. *Yeast* **2004**, *21*, 265–276. [[CrossRef](#)]
- Gomez-Gil, L.; Camara Almiron, J.; Rodriguez Carrillo, P.L.; Olivares Medina, C.N.; Bravo Ruiz, G.; Romo Rodriguez, P.; Corrales Escobosa, A.R.; Gutierrez Corona, F.; Roncero, M.I. Nitrate assimilation pathway (NAP): Role of structural (nit) and transporter (*ntr1*) genes in *Fusarium oxysporum* f.sp. *lycopersici* growth and pathogenicity. *Curr. Genet.* **2018**, *64*, 493–507.
- Khanal, S.; Schroeder, L.; Nava-Mercado, O.A.; Mendoza, H.; Perlin, M.H. Role for nitrate assimilatory genes in virulence of *Ustilago maydis*. *Fungal Biol.* **2021**, *125*, 764–775. [[CrossRef](#)]
- López-Bucio, J.; Esparza-Reynoso, S.; Pelagio-Flores, R. Nitrogen availability determines plant growth promotion and the induction of root branching by the probiotic fungus *Trichoderma atroviride* in *Arabidopsis* seedlings. *Arch. Microbiol.* **2022**, *204*, 380. [[CrossRef](#)] [[PubMed](#)]
- Cao, Y.; Zhu, X.; Jiao, R.; Xia, Y. The *Magas1* gene is involved in pathogenesis by affecting penetration in *Metarhizium acridum*. *J. Microbiol. Biotechnol.* **2012**, *22*, 889–893. [[CrossRef](#)]

15. Jin, K.; Ming, Y.; Xia, Y.X. *MaHog1*, a Hog1-type mitogen-activated protein kinase gene, contributes to stress tolerance and virulence of the entomopathogenic fungus *Metarhizium acridum*. *Microbiology* **2012**, *158*, 2987–2996. [[CrossRef](#)]
16. Wen, Z.; Tian, H.; Xia, Y.; Jin, K. MaPmt1, a protein O-mannosyltransferase, contributes to virulence through governing the appressorium turgor pressure in *Metarhizium acridum*. *Fungal Genet. Biol.* **2020**, *145*, 103480. [[CrossRef](#)]
17. Du, Y.; Jin, K.; Xia, Y. Involvement of MaSom1, a downstream transcriptional factor of cAMP/PKA pathway, in conidial yield, stress tolerances, and virulence in *Metarhizium acridum*. *Appl. Microbiol. Biotechnol.* **2018**, *102*, 5611–5623. [[CrossRef](#)] [[PubMed](#)]
18. Cai, Q.; Wang, J.J.; Xie, J.T.; Jiang, D.H. Functional characterization of BbEaf6 in *Beauveria bassiana*: Implications for fungal virulence and stress response. *Virulence* **2024**, *15*, 2387172. [[CrossRef](#)]
19. Zhang, J.J.; Jiang, H.; Du, Y.; Keyhani, N.O.; Xia, Y.; Jin, K. Members of chitin synthase family in *Metarhizium acridum* differentially affect fungal growth, stress tolerances, cell wall integrity and virulence. *PLoS Pathog.* **2019**, *15*, e1007964. [[CrossRef](#)]
20. Sano, M. *Aspergillus oryzae* nrtA affects kojic acid production. *Biosci. Biotechnol. Biochem.* **2016**, *80*, 1776–1780. [[CrossRef](#)] [[PubMed](#)]
21. Pérez, M.D.; González, C.; Avila, J.; Brito, N.; Siverio, J.M. The YNT1 gene encoding the nitrate transporter in the yeast *Hansenula polymorpha* is clustered with genes YNI1 and YNR1 encoding nitrite reductase and nitrate reductase, and its disruption causes inability to grow in nitrate. *Biochem. J.* **1997**, *321 Pt 2*, 397–403. [[CrossRef](#)] [[PubMed](#)]
22. Gao-Rubinelli, F.; Marzluf, G.A. Identification and characterization of a nitrate transporter gene in *Neurospora crassa*. *Biochem. Genet.* **2004**, *42*, 21–34. [[CrossRef](#)] [[PubMed](#)]
23. Snoeijers, S.S.; Pérez-García, A.; Joosten, M.H.; De Wit, P.J.G.M. The effect of nitrogen on disease development and gene expression in bacterial and fungal plant pathogens. *Eur. J. Plant Pathol.* **2000**, *106*, 493–506. [[CrossRef](#)]
24. Tudzynski, B. Nitrogen regulation of fungal secondary metabolism in fungi. *Front. Microbiol.* **2014**, *5*, 656. [[CrossRef](#)] [[PubMed](#)]
25. Marzluf, G.A. Genetic regulation of nitrogen metabolism in the fungi. *Microbiol. Mol. Biol. Rev.* **1997**, *61*, 17–32. [[PubMed](#)]
26. Wong, K.H.; Hynes, M.J.; Todd, R.B.; Davis, M.A. Transcriptional control of nmrA by the bZIP transcription factor MeaB reveals a new level of nitrogen regulation in *Aspergillus nidulans*. *Mol. Microbiol.* **2007**, *66*, 534–551. [[CrossRef](#)]
27. Ravagnani, A.; Gorfinkiel, L.; Langdon, T.; Diallinas, G.; Adjadj, E.; Demais, S.; Gorton, D.; Arst, H.N.; Scazzocchio, C. Subtle hydrophobic interactions between the seventh residue of the zinc finger loop and the first base of an HGATAR sequence determine promoter-specific recognition by the *Aspergillus nidulans* GATA factor AreA. *EMBO J.* **1997**, *16*, 3974–3986. [[CrossRef](#)] [[PubMed](#)]
28. Burger, G.; Tilburn, J.; Scazzocchio, C. Molecular cloning and functional characterization of the pathway-specific regulatory gene *nirA*, which controls nitrate assimilation in *Aspergillus nidulans*. *Mol. Cell. Biol.* **1991**, *11*, 795–802.
29. Pan, H.; Feng, B.; Marzluf, G.A. Two distinct protein-protein interactions between the NIT2 and NMR regulatory proteins are required to establish nitrogen metabolite repression in *Neurospora crassa*. *Mol. Microbiol.* **1997**, *26*, 721–729. [[CrossRef](#)] [[PubMed](#)]
30. Huberman, L.B.; Wu, V.W.; Kowbela, D.J.; Lee, J.; Daum, C.; Grigorieva, I.V.; O'Malley, R.C.; Glassa, N.L. DNA affinity purification sequencing and transcriptional profiling reveal new aspects of nitrogen regulation in a filamentous fungus. *Proc. Natl. Acad. Sci. USA* **2021**, *118*, e2009501118. [[CrossRef](#)]
31. Berger, H.; Basheer, A.; Bock, S.; Reyes-Dominguez, Y.; Dalik, T.; Altmann, F.; Strauss, J. Dissecting individual steps of nitrogen transcription factor cooperation in the *Aspergillus nidulans* nitrate cluster. *Mol. Microbiol.* **2008**, *69*, 1385–1398. [[CrossRef](#)] [[PubMed](#)]
32. Kotaka, M.; Johnson, C.; Lamb, H.K.; Hawkins, A.R.; Ren, J.; Stammers, D.K. Structural analysis of the recognition of the negative regulator NmrA and DNA by the zinc finger from the GATA-type transcription factor AreA. *J. Mol. Biol.* **2008**, *381*, 373–382. [[CrossRef](#)]
33. Wang, Z.L.; Jin, K.; Xia, Y.X. Transcriptional analysis of the conidiation pattern shift of the entomopathogenic fungus *Metarhizium acridum* in response to different nutrients. *BMC Genom.* **2016**, *17*, 586. [[CrossRef](#)] [[PubMed](#)]
34. Li, C.C.; Xu, D.X.; Hu, M.W.; Zhang, Q.P.; Xia, Y.X.; Jin, K. MaNCP1, a C2H2 zinc finger protein, governs the conidiation pattern shift through regulating the reductive pathway for nitric oxide synthesis in the filamentous fungus *Metarhizium acridum*. *Microbiol. Spectr.* **2022**, *10*, e00538-22. [[CrossRef](#)] [[PubMed](#)]
35. Li, C.C.; Xia, Y.X.; Jin, K. The C2H2 zinc finger protein MaNCP1 contributes to conidiation through governing the nitrate assimilation pathway in the entomopathogenic fungus *Metarhizium acridum*. *J. Fungi* **2022**, *8*, 942. [[CrossRef](#)] [[PubMed](#)]
36. Zhao, Y.X.; Lim, J.Y.; Xu, J.Y.; Yu, J.H.; Zheng, W. Nitric oxide as a developmental and metabolic signal in filamentous fungi. *Mol. Microbiol.* **2020**, *113*, 872–882. [[CrossRef](#)]
37. Unkles, S.E.; Zhuo, D.; Siddiqi, M.Y.; Kinghorn, J.R.; Glass, A.D.M. Apparent genetic redundancy facilitates ecological plasticity for nitrate transport. *EMBO J.* **2001**, *22*, 6246–6255. [[CrossRef](#)]
38. Li, C.C.; Xia, Y.X.; Jin, K. N-terminal zinc fingers of MaNCP1 contribute to growth, stress tolerance, and virulence in *Metarhizium acridum*. *Int. J. Biol. Macromol.* **2022**, *216*, 426–436. [[CrossRef](#)]
39. Li, C.C.; Zhang, Q.P.; Xia, Y.X.; Jin, K. MaNmrA, a negative transcription regulator in nitrogen catabolite repression pathway, contributes to nutrient utilization, stress resistance and virulence in entomopathogenic fungus *Metarhizium acridum*. *Biology* **2021**, *10*, 1167. [[CrossRef](#)] [[PubMed](#)]
40. Xie, X.Q.; Li, F.; Ying, S.H.; Feng, M.G. Additive contributions of two manganese-cored superoxide dismutases (MnSODs) to antioxidation, UV tolerance and virulence of *Beauveria bassiana*. *PLoS ONE* **2012**, *7*, e30298. [[CrossRef](#)]

41. Ibe, C.; Munro, C.A. Fungal cell wall proteins and signaling pathways form a cytoprotective network to combat stresses. *J. Fungi* **2021**, *7*, 739. [[CrossRef](#)]
42. Perez-Nadales, E.; Di Pietro, A. The transmembrane protein Sho1 cooperates with the mucin Msb2 to regulate invasive growth and plant infection in *Fusarium oxysporum*. *Mol. Plant Pathol.* **2015**, *16*, 593–603. [[CrossRef](#)] [[PubMed](#)]
43. Ram, A.F.; Klis, F.M. Identification of fungal cell wall mutants using susceptibility assays based on Calcofluor white and Congo red. *Nat. Protoc.* **2006**, *1*, 2253–2256. [[CrossRef](#)]
44. Landi, S.; Esposito, S. Nitrate Uptake Affects Cell wall synthesis and modeling. *Front. Plant Sci.* **2017**, *8*, 1376. [[CrossRef](#)] [[PubMed](#)]
45. Pfannmüller, A.; Boysen, J.M.; Tudzynski, B. Nitrate assimilation in *Fusarium fujikuroi* is controlled by multiple levels of regulation. *Front. Microbiol.* **2017**, *8*, 381. [[CrossRef](#)]
46. Gardiner, D.M.; Kazan, K.; Manners, J.M. Nutrient profiling reveals potent inducers of trichothecene biosynthesis in *Fusarium graminearum*. *Fungal Genet. Biol.* **2009**, *46*, 604–613. [[CrossRef](#)] [[PubMed](#)]
47. Qi, Y.X.; Chen, F.X.; Li, Z.Z. Effects of carbon sources and nitrogen sources on the biological characteristics and antifungal activity of *Beauveria bassiana*. *Acta Laser Biol. Sin.* **2011**, *20*, 38–44.
48. Liu, Y.; Li, Y.X.; Tong, S.; Wang, J.Y.; Zhu, S.A.; Zhang, L.Y.; Fan, Y.H. Effects of *NirA1* gene on growth, stress resistance and virulence of *Beauveria bassiana*. *Acta Microbiol. Sin.* **2021**, *61*, 2469–2480.
49. Brown, N.A.; Urban, M.; Van de Meene, A.M.L.; Hammond-Kosack, K.E. The infection biology of *Fusarium graminearum*: Defining the pathways of spikelet to spikelet colonisation in wheat ears. *Fungal Biol.* **2010**, *114*, 555–571. [[CrossRef](#)]
50. Horowitz, S.; Freeman, S.; Zveibil, A.; Yarden, O. A defect in *nir1*, a *nirA*-like transcription factor, confers morphological abnormalities and loss of pathogenicity in *Colletotrichum acutatum*. *Mol. Plant Pathol.* **2006**, *7*, 341–354. [[CrossRef](#)]
51. Wilson, R.A.; Jenkinson, J.M.; Gibson, R.P.; Littlechild, J.A.; Wang, Z.Y.; Talbot, N.J. *Tps1* regulates the pentose phosphate pathway, nitrogen metabolism and fungal virulence. *EMBO J.* **2007**, *26*, 3673–3685. [[CrossRef](#)] [[PubMed](#)]
52. Wilson, R.A.; Gibson, R.P.; Quispe, C.F.; Littlechild, J.A.; Talbot, N.J. An NADPH-dependent genetic switch regulates plant infection by the rice blast fungus. *Proc. Natl. Acad. Sci. USA* **2010**, *107*, 21902–21907. [[CrossRef](#)] [[PubMed](#)]
53. Marroquin-Guzman, M.; Wilson, R.A. GATA-dependent glutaminolysis drives appressorium formation in *Magnaporthe oryzae* by suppressing TOR inhibition of cAMP/PKA signaling. *PLoS Pathog.* **2015**, *11*, e1004851. [[CrossRef](#)] [[PubMed](#)]
54. Li, G.; Gong, Z.; Dulal, N.; Marroquin-Guzman, M.; Rocha, R.O.; Richter, M.; Wilson, R.A. A protein kinase coordinates cycles of autophagy and glutaminolysis in invasive hyphae of the fungus *Magnaporthe oryzae* within rice cells. *Nat. Commun.* **2023**, *14*, 4146. [[CrossRef](#)]
55. Li, C.C.; Zhang, Q.P.; Xia, Y.X.; Jin, K. MaAreB, a GATA transcription factor, is involved in nitrogen source utilization, stress tolerances and virulence in *Metarhizium acridum*. *J. Fungi* **2021**, *7*, 512. [[CrossRef](#)] [[PubMed](#)]
56. van de Veerdonk, F.L.; Gresnigt, M.S.; Romani, L.; Romani, L.; Netea, M.G.; Latgé, J.P. *Aspergillus fumigatus* morphology and dynamic host interactions. *Nat. Rev. Microbiol.* **2017**, *15*, 661–674. [[CrossRef](#)] [[PubMed](#)]
57. Wang, G.; Xu, S.; Chen, L.; Zhan, T.; Zhang, X.; Liang, H.; Chen, B.; Peng, Y. Gut microbial diversity reveals differences in pathogenicity between *Metarhizium rileyi* and *Beauveria bassiana* during the early stage of infection in *Spodoptera litura* larvae. *Microorganisms* **2024**, *12*, 1129. [[CrossRef](#)]
58. Jin, K.; Peng, G.X.; Liu, Y.C.; Xia, Y.X. The acid trehalase, ATM1, contributes to the in vivo growth and virulence of the entomopathogenic fungus, *Metarhizium acridum*. *Fungal Genet. Biol.* **2015**, *77*, 61–67. [[CrossRef](#)] [[PubMed](#)]
59. Wang, C.S.; St Leger, R.J. A collagenous protective coat enables *Metarhizium anisopliae* to evade insect immune responses. *Proc. Natl. Acad. Sci. USA* **2006**, *103*, 6647–6652. [[CrossRef](#)]

**Disclaimer/Publisher’s Note:** The statements, opinions and data contained in all publications are solely those of the individual author(s) and contributor(s) and not of MDPI and/or the editor(s). MDPI and/or the editor(s) disclaim responsibility for any injury to people or property resulting from any ideas, methods, instructions or products referred to in the content.